Korean J. Chem. Eng., **22**(1), 154-160 (2005)

Influence of Hydrodynamic Parameters on Particle Attrition during Fluidization at High Temperature

Chiou-Liang Lin and Ming-Yen Wey†

Department of Environmental Engineering, National Chung-Hsing University, Taichung, 402, Taiwan, ROC
(*Received 26 July 2004 • accepted 11 October 2004*)

Abstract−In a fluidized bed, attrition both increases the number of particles and reduces particle size, which may affect reactor performance, fluidizing properties, operating stability and operating costs. Most fluidized applications are conducted at high temperature, but in the past most attrition correlations were performed at room temperature, so the attrition rate at high temperature could not be predicted. In contrast, this study investigates the attrition rate of fluidized materials at high temperature. Silica sand was used as the bed material; the operating parameters included temperature, particle size, static bed height and gas velocity to assess the attrition rate. Then an appropriate correlation was developed by regression analysis to predict attrition rate at high temperature. Experimental results indicated that the attrition rate increases with increasing temperature. In addition, the particle attrition increased as average particle size decreased because the probability of collision increases with surface area. The attrition rate increased with increasing gas velocity because of increased kinetic stress of particle movement. The actual density and viscosity of air at specific fluidization temperature were modified and an Ar number was introduced to fit our experimental data. The experimental correction agrees with the experimental results, which can predict particle attrition rate at high temperatures.

Key words: Gas-solid Fluidization, Attrition Rate, High Temperature

INTRODUCTION

Fluidized bed reactors are the most widespread owing to such advantages as good solid mixing, high heat transfer and large contact surface area [Jang et al., 2002]. They have been employed in many industrial processes, such as combustion [Jang et al., 2003], drying [Choi et al., 2002], catalysis [Lee et al., 2003], gasification [Lee et al., 2002], separation [Lee and Shin, 2003], photocatalytic oxidation [Lim and Kim, 2004; Kim et al., 2004; Na et al., 2004] and others. Evaluating particle attrition is important in many fluidized bed systems. Because attrition increases the number of particles and reduces particle size, which may affect reactor performance, fluidizing properties, operating stability and operating costs [Bemrose and Bridgwater, 1987]. In addition, the load of air pollution control devices is increased in order to collect the fine particles carried with flue gas from a chamber.

The particle attrition rate is affected in many ways. Lee et al. [1993] indicated that porosity, size, hardness, density, surface, cracks and shape all affect the attrition rate. Additionally, Bemrose and Bridgwater [1987] showed that the reactor environment characteristics which influence attrition include the particle velocity, exposure time, temperature and pressure. According to Arena et al. [1983], the attrition rate constant is affected by the size of sand and by bed temperature. Ulerich et al. [1980], Vaux and Fellers [1981] and Ayazi Shamlou et al. [1990] gathered previous results to show that attrition of the fluidized bed was caused by several mechanisms, including chemical stress, thermal stress, kinetic stress and static stress.

Previous investigations corrected their experimental data to develop empirical correlations in different operating conditions, in order to predict the particle attrition rate. Table 1 lists previous correlations for different conditions. However, these correlation results were a significantly different, because the authors used different operating parameters. Merrick and Highley [1974] found that the elutriation rate of ash particles was proportional to the excess gas velocity. Additionally, Vaux and Schruben [1978], Lin et al. [1980], Ulerich et al. [1980] and Ayazi Shamlou et al. [1990] also found the same results, although they showed the rate of attrition to be a function of excess gas velocity. Wu et al. [1999] used silica sand as the fluidized material, and showed that particle attrition increased with increasing bed weight, Merrick and Highley [1974] and Donsí et al. [1981] also showed that particle attrition rate is proportional to the static bed height, and that attrition rate increases with decreasing average particle size. This is because smaller particles represent a larger number of particles for the same weight basis and have a larger surface area, which increases the probability of collision [Wu et al., 1999; Ray and Jiang 1987].

Most fluidized applications are conducted at high temperature, but since most attrition correlations were performed at room temperature, they could not predict the attrition rate at high temperature. However, previous research focused less on the effect of temperature on particle attrition rate. This study investigates the attrition rate of fluidized materials at high temperature. The operating parameters include temperature, particle size, static bed height and gas velocity to assess particle attrition rate. Then an appropriate correlation is developed by regression analysis to predict attrition rate at high temperature.

EXPERIMENTAL

Lin and Wey [2003] discuss the effect of temperature and combustion conditions on attrition at high temperature. Comparing ex-

†To whom correspondence should be addressed.
E-mail: mywey@dragon.nchu.edu.tw

Table 1. Predicted equations of previous researches

Author	Operating conditions	Attrition rate equation		Patricle
Gwyn [1969]	*Particle size (51-260 μm) *Room temperature	$R_t = K_p \times m \times t^{m-1} \times W$	$m = 0.46$ $K_P = 4.47\times10^{-6} \sim 1.35\times10^{-5}$	Silica sand
Merrick and Highely [1974]	*Gas velocity (0.6-2.4 m/s) *Bed height (0.6-1.2 m) *Particle size (1,587-3,175 μm)	$R_t = K_a \times (U_0 - U_{mf}) \times W$	$K_a = 4.54\times10^{-3} \sim 0.015$	Limestone
Kono [1981]	*Particle size (970-4,000 μm) *U/U_{mf} (1.5-5) *Temperature (298-777 K)	$R_t = 2.43\times10^{-9} \times \rho_f \times \overline{U}^3 \times D_t^{0.55} \times W$ $R_t = 8.85\times10^{-9} \times \rho_f \times \overline{U}^2 \times D_t^{0.55} \times W$	For $\overline{U} \le 3.6$ m/s For $\overline{U} > 3.6$ m/s	Silica sand
Halder and Basu [1992]	*Gas velocity (1.7-3.77 m/s) *Temperature (300, 1,073 K) *Sand size (212-355 μm)	$R_t = K_a U_0 W / d_p$	$K_a = 2.57 \sim 4.8\times10^{-7}$ combustion $K_a = 0.03 \sim 0.05\times10^{-7}$ absence combustion condition	Carbon
Lee et al. [1993]	*Gas velocity (2-5 m/s) *Temperature (293-450 K) *Particle size (820, 1,682 μm)	$W_e = (W - W_{min}) \times e^{-K_a t} + W_{min}$ $K_a = K_0 \exp\left[-\frac{E_a RTC_{s,crit}}{PM_W U_0 (U_0 - U_{mf})}\right]$	$E_a = 3.383\times10^{-3}$ kJ/kg $K_0 = 1.29\times10^{-4}$ s^{-1}	Lime
Cook et al. [1996]	*Gas velocity (1.54-5.0 m/s) *Particle size (903, 1,764 μm)	$R_t = K_a \times \exp[-E_a/(U_0 - U_{mf})^2] \times W$	$E_a = 3.969\times10^{-2}$ kJ/kg $K_a = 2.89\times10^{-6}$ s^{-1}	Lime
Wu et al. [1999]	*Particle size (195-421 μm) *Nozzle size (0.003-0.005 m) *Gas velocity (0.4-1.1 m/s)	$R_t = K_{a0} \times U_0 (U_0 - U_{mf}) \times W/(g \times d_{sv})$ $R_t = K^*_{a0} \times U_0 \times (Q_B/A) \times W$	$K_{a0} = 7.4\times10^{-3}$ s^{-1} $K^*_{a0} = 2.5\times10^{-7}$ s/m^2	Silica sand
Chu et al. [2000]	*Particle size (210-500 μm) *Temperature (313-338 K) *Gas velocity (0.17-0.3 m/s)	$W_e = W_{c0} \times [1 - \exp(-K_a \int_0^t (1 - X_s) dt)]$	$K_a = 1.63\times10^{-2}(U_0/d_{pc})$	Limestone
Park et al. [2000]	*Particle size (1,400-1,700 μm) *$U - U_{mf}$ (0.05-0.5 m/s) *Bed height (0.11-0.25 m) *Bed weight (0.6-1.4 kg)	$R_t = 0.01443(U_0 - U_{mf})W - 142.91$		Alumina

perimental data with previous correlations reveals a significant level of error in the predicted results from existing correlations. In order to predict the attrition rate at high temperature, the various parameters were tested continually to regress an experimental correlation. The experimental apparatus for this study is shown in Fig. 1. The reactor was a bubbling fluidized bed, consisting of a preheated chamber, a main chamber and an expansion section. The preheated chamber was 0.5 m long. The main chamber was 1.1 m high and 0.09 m in diameter. The expansion section was 1.0 m high and 0.25 m in diameter. The reactor was equipped with a stainless steel porous plate that had a 15% open area to provide gas distribution, and was surrounded by electric resistance elements and packed with ceramic fiber to insulate heat loss. Three thermocouples were used to measure the temperature profile in the preheated chamber, sand bed, and freeboard chamber. The thermocouples send the feedback signal of temperature to the PID controller. The PID controller maintains the experimental temperature by controlling the electric resistance. The elutriation particles were collected by two cyclones and a bag filter. Silica sand was used as the bed material, and had nearly the same density for all sizes (ρ_p=2.6 g/cm^3). The operating parameters included temperature (298-1,173 K), particle size (385-1,095 μm), static bed height (1.2-2.0 H/D) and gas velocity (0.14-0.29 m/s) to assess particle attrition rate. Table 2 lists the operating parameters of this investigation. These experiments were carried out at atmospheric pressure.

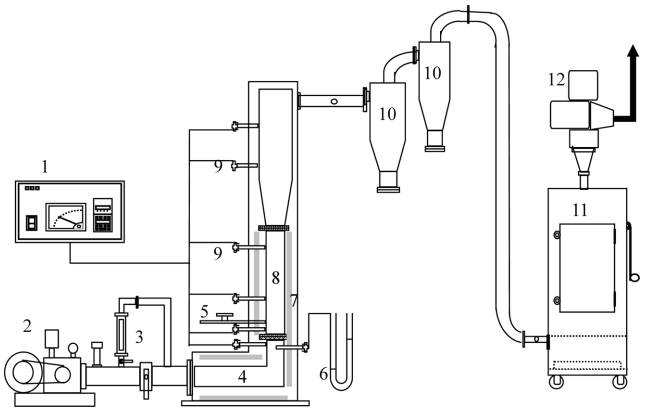

Fig. 1. The bubble fluidized bed incinerator.

1. PID controller
2. Blower
3. Flow meter
4. Preheater chamber
5. Feeder
6. U manometer
7. Electric resistance
8. Sand bed
9. Thermocouple
10. Cyclone
11. Bag filter
12. Induced fan

The reactor chamber was heated by an electrical heater, and the experimental procedure started by preheating the sand bed to the

Table 2. The operating conditions for each experiment

Run	Temperature (°C)	Particle size (μm)	Static bed height (H/D)	Gas velocity (m/s)	Operating time (sec)
1	25	770	2.0	0.18	0-14,400
2	100	770	2.0	0.18	0-14,400
3	200	770	2.0	0.18	0-14,400
4	300	770	2.0	0.18	0-14,400
5	400	770	2.0	0.18	0-14,400
6	500	770	2.0	0.18	0-14,400
7	600	770	2.0	0.18	0-14,400
8	700	770	2.0	0.18	0-14,400
9	800	770	2.0	0.18	0-14,400
10	900	770	2.0	0.18	0-14,400
11	800	385	2.0	0.18	0-14,400
12	800	460	2.0	0.18	0-14,400
13	800	545	2.0	0.18	0-14,400
14	800	645	2.0	0.18	0-14,400
15	800	770	2.0	0.18	0-14,400
16	800	920	2.0	0.18	0-14,400
17	800	1,095	2.0	0.18	0-14,400
18	800	770	2.0	0.14	0-14,400
19	800	770	2.0	0.18	0-14,400
20	800	770	2.0	0.21	0-14,400
21	800	770	2.0	0.25	0-14,400
22	800	770	2.0	0.29	0-14,400
23	800	770	1.2	0.18	0-14,400
24	800	770	1.4	0.18	0-14,400
25	800	770	1.6	0.18	0-14,400
26	800	770	1.8	0.18	0-14,400
27	800	770	2.0	0.18	0-14,400

operating temperature. The hot air was flowed into the bed, and the attrition of materials began. At the initial step of every experiment run, the reactor was stopped every 600 sec and cooled for 25,200 sec. When the sand bed had cooled to room temperature, the residual bed materials were collected and elutriation particles were also collected by the cyclones and bag filter. These residual bed materials were weighed and these were put into the reactor after weighing. Then, the above steps were repeated and after three times (total attrition time was 1,800 sec) were stopped every 1,800 sec. The total attrition time was 14,400 sec. The attrition rate was assumed to be the same as the elutriation rate because the terminal velocity of the particles always exceeded the superficial gas velocity in this experiment. In previous studies Chu et al. [2000] used this assumption.

According to a previous study [Wu and Chu, 1998], the attrition rate was determined by the material balance for fine particles as follows:

(Initial input, actual generation)=Output+Accumulation

$$F_{0(fine)} = F_{2(fine)} + \frac{dW_{(fine)}}{dt} \quad (1)$$

Solving the above equation gives the weight of fines in the bed as a function of time:

$$W_{(fine)} = \frac{F_{0(fine)}}{K_{(fine)}}[1 - e^{-K_{(fine)}t}] + W_{0(fine)} e^{-K_{(fine)}t} \quad (2)$$

The total carryover balance of fines

total carryover=(initially in bed)+(flow in from t=0)−(in bed at time t)

Rearranging the above equation gives the fines in the carryover stream; therefore, the equation was defined as:

$$W_{(fine\ in\ carryover)} = \left[W_{0(fine)} - \frac{F_{0(fine)}}{K_{(fine)}}\right] \cdot [1 - e^{-K_{(fine)}t}] + F_{0(fine)}t \quad (3)$$

Where $K_{(fine)}$, $W_{0(fine)}$ and $F_{0(fine)}$ are unknowns that can be found by the slope and intercept of a typical experiment. The typical figure was shown as Lin and Wey [2003]. According to this figure, the final slope was the attrition rate. So, we can refer to this method to paint the accumulation loss weight of sand with attrition time and obtain the final slope of this curve to determine the attrition rate.

RESULTS AND DISCUSSION

1. The Effect of High Temperature on Particle Attrition Rate

Fig. 2 shows that the particle attrition rate increases with increasing temperature as the operating temperature rises from 298 K to 1,173 K; this is due to thermal stress since heating particles to an unequal temperature causes uneven expansion and the possibility of decrepitation. At high temperatures, the minimum fluidization velocity decreases with increasing temperature [Wu et al., 1991; Lin et al., 2002]. Particles move faster at high temperatures than at

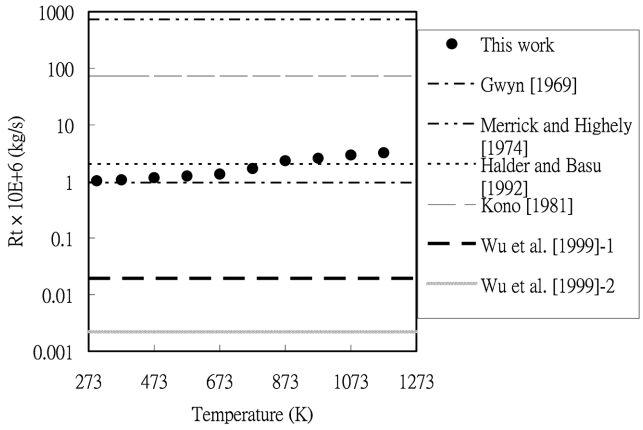

Fig. 2. The results of predicted compared with experimental attrition rate of different operating temperature (particle size= 770 μm, gas velocity=0.18 m/s and H/D=2.0).

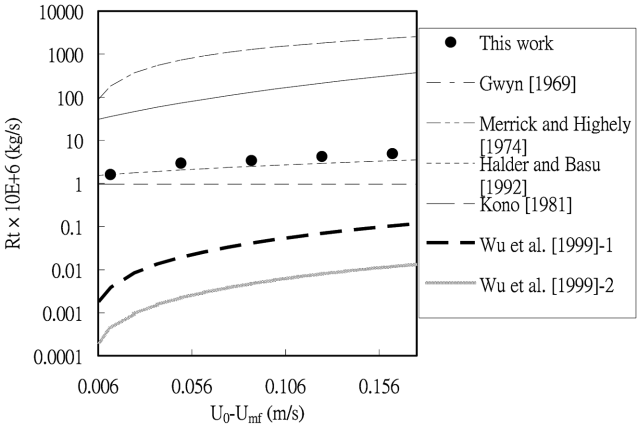

Fig. 4. The results of predicted compared with experimental attrition rate of different gas velocity (particle size=770 μm, temperature=1,073 K and H/D=2.0).

low temperatures with the same air flow rate. Therefore, the thermal and kinetic stress at high operating temperature causes the increase of particle attrition.

To predict particle attrition rate, previous investigations corrected their experimental data to develop empirical correlations in different operating conditions, as listed in Table 1. However, most attrition correlations were performed at room temperature, which could not consider the influence of temperature. In order to compare the experimental data in our study with predicted values, operating parameters were introduced to calculate the predicted values. Fig. 2 shows that the predicted values compared with the attrition rate measured by this investigation at high temperature. It can be seen that particle attrition rate increases with increasing temperature, but the attrition rate of correlations does not increase with temperature. Although Gwyn [1969], Kono [1981] and Wu et al. [1999] used silica sand as the bed material, their experimental correlations had a significant level of error. These may be due to the fact that previous researchers neglected the effect of temperature on attrition.

2. Effect of Particle Size on Particle Attrition Rate

According to Table 1, most correlations did not consider the influence of particle size, such as Gwyn [1969], Merrick and Highely [1974] and Kono [1981]. Therefore, these predicted values maintain constant at different particle size. However, Fig. 3 shows that particle attrition increased with decreasing average particle size. This is because smaller particles have a larger number of particles for the same weight basis with a larger surface area, which increases the probability of collision [Wu et al., 1999; Ray and Jiang, 1987]. Ray and Jiang [1987] developed a "surface-reaction" model and indicated that particle attrition is proportional to particle surface area. The particle attrition rate is larger for fine particles than for coarse particles. Additionally, the minimum fluidization velocity of fine particles is smaller than of large particles at the same temperature. Consequently, fine particles move faster at the same gas velocity to increase kinetic stress, which affects the attrition rate. Therefore, the probability of particle collision increases to raise attrition rate.

3. Effect of Gas Velocity and Static Bed Height on Particle Attrition Rate

Fig. 4 displays the attrition rate at different gas velocity. The attrition rate increases with gas velocity, because kinetic stress increases as particles move faster, thus increasing the rate of particle collision and attrition. Comparing the calculation results of correlation with experimental data at different gas velocities and 1,073 K, both

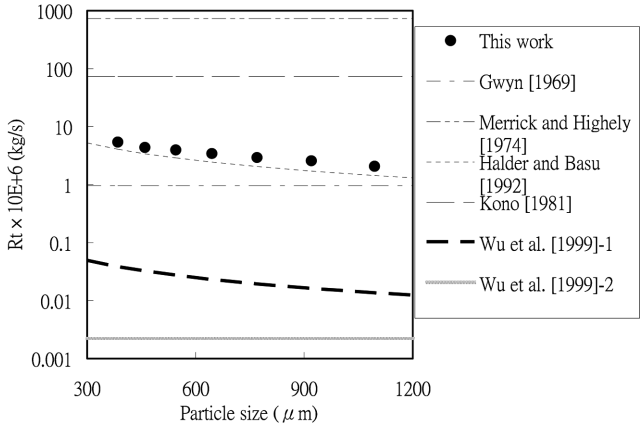

Fig. 3. The results of predicted compared with experimental attrition rate of different particle size (temperature=1,073 K, gas velocity=0.18 m/s and H/D=2.0).

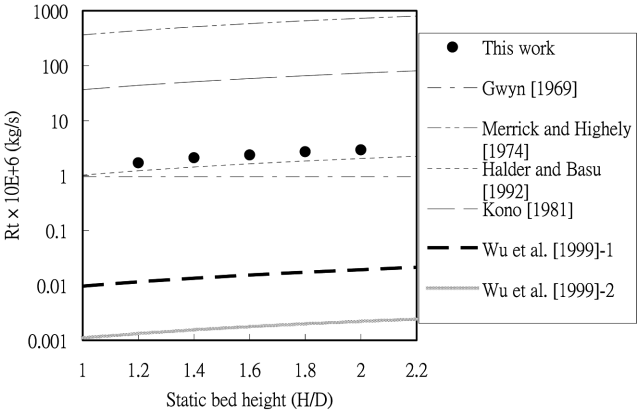

Fig. 5. The results of predicted compared with experimental attrition rate of different static bed height (particle size=770 μm, temperature=1,073 K and gas velocity=0.18 m/s).

values have the same trend. The attrition rate increases with gas velocity, but these results of equations have a level of error in the prediction. This result may be due to the operating temperature.

Fig. 5 illustrates the effect of bed height on attrition rate; the attrition rate increases with static bed height. In a deeper bed, a rising bubble has a longer residence time and may coalesce with other bubbles while rising, increasing the fluctuation of bed materials. The bubble fluctuation increases the collisions of moving particles and improves the attrition rate of sand. Additionally, the weight of bed materials increases with increasing static bed height. Therefore, the static stress (particle gravity) increases to cause attrition rate to rise. Fig. 5 also shows the calculation results and compares them with the experimental data at different static bed heights. The bed weight plays an important role in these correlations. But these equations don't predict attrition rate well. This error may occur because the previous correlations neglected the effect of operating temperature, which concerned gas velocity and the weight of bed.

4. Development of a More Appropriate Correlation

According to previous research, many operating parameters affect particle attrition rate, but most investigators developed their empirical correlations based on the gas velocity, and neglected the effect of temperature, particle size and particle properties. However, gas velocity is not the only important parameter in predicting attrition rate. The particle size and operating temperature are also important, as shown in Figs. 2-4. These previous correlation results have a significant level of difference because the experimental equations neglected many parameters, such as particle size, operating temperature and particle properties.

To predict the particle attrition at high temperature, the operating temperature was used as major parameter. Particle size, static bed height and gas velocity were changed to investigate particle attrition rate. According to experimental data, the attrition rate can be defined as:

$$\text{Attrition rate (Rt)} \approx t\left[\begin{array}{l}\text{excess gas velocity, particle size,}\\ \text{weight of bed, Ar number}\end{array}\right]$$

For fluidized bed systems, the Ar number is a general parameter to calculate the fluidization characteristics. Because the Ar number is composed of density and viscosity of air, our regression analysis introduced a variable Ar number to fit experimental data. However, for previous studies, the density and viscosity of air was a constant at room temperature. In order to show the effect of temperature on attrition, the actual density and viscosity of air was modified to represent the influence of temperature. The actual and specific fluidization temperature was modified by the Svoboda and Hartman [1981] relations.

$$\rho_g = 1.2\frac{293}{T} \tag{4}$$

$$\mu_g = \frac{1.46\times10^{-6}T^{1.504}}{T+120} \tag{5}$$

All experimental data have been transformed to fit experimental correlation. Then the order of parameter and unit were calculated by regression analysis to predict the attrition rate at high temperature. The experimental correlation is Eq. (6).

$$Rt = k_0\left[\frac{(U_0-U_{mf})d_P}{Ar\mu_g}\right]^{1/2}\frac{W^{3/2}}{A} \tag{6}$$

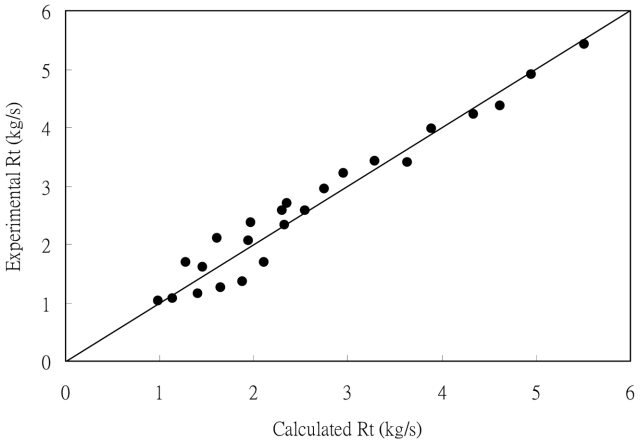

Fig. 6. Comparing experimental results with regression correlation.

From curve fitting, the proportionality coefficient k_0 was defined as:

$$k_0 = 0.2423\times10^{-6}, \left(\frac{m^{0.5}}{s}\right)$$

The fitting results are represented in Fig. 6 and experimental results can be predicted well. The correlation coefficient was 0.95. Therefore, the particle attrition rate can be predicted well at different operating conditions, such as temperature, particle size and gas velocity.

CONCLUSION

This study investigates the attrition rate of fluidized materials under different conditions. The considered parameters include operating temperature, particle size, static bed height and gas velocity. The measurement results demonstrate that particle attrition increases as temperature increases because the thermal stress increases with increasing temperature. The attrition rate also increases as particle size decreases because the probability of collision increases with surface area. Furthermore, attrition also increases with operating gas velocity, because the kinetic stress increases.

Most previous investigators developed their empirical correlations based on the gas velocity, and neglected the effect of temperature and particle size. According to these experimental results, the temperature and particle size play important roles for particle attrition. Therefore, the regression analysis introduces the actual density and viscosity of air, which was modified to represent the influence of temperature, and which uses a variable Ar number to fit experimental data. The particle attrition can be predicted well for different operating temperatures, particle sizes and gas velocities.

NOMENCLATURE

A : cross-sectional area of the bed [m^2]
Ar : Archimedes number, $\frac{d_P^3\rho_g(\rho_P-\rho_g)g}{\mu_g^2}$ [-]
$C_{s,crit}$: critical weight of solid [kg]
d_p : average particle diameter[m]
d_{pc} : the average particle diameter of sorbent [m]

d_{sv} : average sieve cut size [m]
D_t : diameter of fluidized bed [m]
E_a : attrition activation energy [kJ/kg]
$F_{0(fine)}$: fictitious feed stream of fines [kg/s]
$F_{2(fine)}$: total fines carried out of the bed since t=0 [kg/s]
g : acceleration due to gravity [m/s^2]
k_0 : attrition rate constant of this work [m$^{0.5}$/s]
K_0 : frequency factor in an Arrhenius form [1/s]
$K_{(fine)}$: elutriation rate constant of fines [1/s]
K_a : attrition rate constant [1/s]
K_{a0} : intrinsic attrition constant [1/s]
K^*_{a0} : intrinsic attrition constant factor [s/m^2]
K_p : dimensional constant, unit t^{-m}, in mass rate equation
m : exponent for time dependence of attrition [-]
M_w : molecular weight of gas [kg/kg-mol]
Q_B : visible bubble volume [m^3/s]
R : gas constant [kJ/kg-molK]
Rt : attrition rate [kg/s]
t : attrition time [s]
T : temperature [K]
$\overline{U}$: effective gas velocity [m/s]
U_0 : superficial gas velocity [m/s]
U_{mf} : minimum fluidization velocity [m/s]
W : weight of bed material [kg]
$W_{0(fine)}$: initial weight of fines in the bed [kg]
W_{c0} : initial weight of the sorbent particles [kg]
W_e : total mass of particles elutriated until time t [kg]
W_{min} : minimum weight of parent solids in a bed [kg]
$W_{(fine\ in\ carryover)}$: total mass of particles carried [kg]
X_s : the conversion of the sorbent in the cyclone [-]
ρ_g : air density [kg/m^3]
ρ_f : density of fluidizing gas [kg/m^3]
ρ_p : solids density [kg/m^3]
μ_g : air viscosity [kg/ms]

REFERENCES

Arena, V., D'Amore, M. and Massimilla, L., "Carbon Attrition during the Fluidized Combustion of a Coal," *AIChE J.*, **29**, 40 (1983).

Ayazi Shamlou, P., Liu, Z. and Yates, J. G., "Hydrodynamic Influences on Particle Breakage in Fluidized Beds," *Chem. Eng. Sci.*, **45**, 809 (1990).

Bemrose, C. R. and Bridgwater, J., "A Review of Attrition and Attrition Test Methods," *Powder Technol.*, **2**, 97 (1987).

Choi, K. B., Park, S. I., Park, Y. S., Sung, S. W. and Lee, D. H., "Drying Characteristics of Millet in a Continuous Multistage Fluidized Bed," *Korean J. Chem. Eng.*, **19**, 1106 (2002).

Chu, C. Y., Hsueh, K. W. and Hwang, S. J., "Sulfation and Attrition of Calcium Sorbent in a Bubbling Fluidized Bed," *J. of Hazardous Materials*, **B80**, 119 (2000).

Cook, L. J., Khang, S. J., Lee, S. K. and Tim, C. K., "Attrition and Changes in Particles Distribution of Lime Sorbents in a Circulation Fluidized Bed Absorber," *Powder Technol.*, **89**, 1 (1996).

Donsí, G., Massimilla, L. and Miccio, M., "Carbon Fines Production and Elutriation from the Bed of a Fluidized Coal Combustor," *Combust. Flame*, **41**, 57 (1981).

Gwyn, J. E., "On the Particle Distribution Function and the Attrition of Cracking Catalysts," *AIChE J.*, **15**, 35 (1969).

Halder, P. K. and Basu, P., "Attrition of Spherical Electrode Carbon Particles During Combustion in a Turbulent Fluidized Bed," *Chem. Eng. Sci.*, **47**, 527 (1992).

Jang, H. T., Kim, S. B., Cha, W. S., Hong, S. C. and Doh, D. S., "Pressure Fluctuation Properties in Combustion of Mixture of Anthracite and Bituminous Coal in a Fluidized Bed," *Korean J. Chem. Eng.*, **20**, 138 (2003).

Jang, J. G., Kim, M. R., Lee, K. H. and Lee, J. K., "Enhancement of Combustion Efficiency with Mixing Ratio during Fluidized Bed Combustion of Anthracite and Bituminous Blended Coal," *Korean J. Chem. Eng.*, **19**, 1059 (2002).

Kim, M. J., Nam, W. and Han, G. Y., "Photocatalytic Oxidation of Ethyl Alcohol in an Annulus Fluidized Bed Reactor," *Korean J. Chem. Eng.*, **21**, 721 (2004).

Kono, H., "Attrition Rate of Relatively Coarse Solid Particles in Various Types of Fluidized Beds," *AIChE Symp. Ser.*, **77**, 96 (1981).

Lee, C. G., Kim, J. S., Song, P. S., Choi, G. S., Kang, Y. and Choi, M. J., "Decomposition Characteristics of Residue from the Pyrolysis of Polystyrene Waste in a Fluidized-Bed Reactor," *Korean J. Chem. Eng.*, **20**, 133 (2003).

Lee, J. K. and Shin, J. H., "Design and Performance Evaluation of Triboelectrostatic Separation System for the Separation of PVC and PET Materials using a Fluidized Bed Tribocharger," *Korean J. Chem. Eng.*, **20**, 572 (2003).

Lee, S. K., Jiang, X., Keener, T. C. and Khang, S. J., "Attrition of Lime Sorbents during Fluidization in a Circulating Fluidized Bed Absorber," *Ind. Eng. Chem. Res.*, **32**, 2758 (1993).

Lee, W. J., Kim, S. D. and Song, B. H., "Steam Gasification of an Australian Bituminous Coal in a Fluidized Bed," *Korean J. Chem. Eng.*, **19**, 1091 (2002).

Lim, T. H. and Kim, S. D., "Photo-degradation Characteristics of TCE (Trichloroethylene) in an Annulus Fluidized Bed Photoreactor," *Korean J. Chem. Eng.*, **21**, 905 (2004).

Lin, C. L. and Wey, M. Y., "Effects of High Temperature and Combustion on Fluidized Materials Attrition in Fluidized Bed," *Korean J. Chem. Eng.*, **20**, 1123 (2003).

Lin, C. L., Wey, M. Y. and You, S. D., "The Effect of Particle Size Distribution on Minimum Fluidization Velocity at High Temperature," *Powder Technol.*, **126**, 297 (2002).

Lin, L., Sesrs, J. T. and Wen C. Y., "Elutriation and Attrition of Char a Large Fluidized Bed," *Powder Technol.*, **27**, 105 (1980).

Merrick, D. and Highley, J., "Particle Size Reduction and Elutriation in a Fluidized Bed Process," *AIChE Symp. Ser.*, **70**, 366 (1974).

Na, Y. S., Kim, D. H., Lee, C. H., Lee, S. W., Park, Y. S., Oh, Y. K., Park, S. H. and Song, S. K., "Photocatalytic Decolorization of Rhodamine B by Fluidized Bed Reactor with Hollow Ceramic Ball Photocatalyst," *Korean J. Chem. Eng.*, **21**, 430 (2004).

Park, Y. S., Kim, H. S., Shun, D., Song, K. S. and Kang, S. K., "Attrition Characteristics of Alumina Catalyst for Fluidized Bed Incinerator," *Korean J. Chem. Eng.*, **17**, 284 (2000).

Ray, Y. C. and Jiang, T. S., "Particle Attrition Phenomena in a Fluidized Bed," *Powder Technol.*, **49**, 193 (1987).

Svoboda, K. and Hartman, M., "Influence of Temperature on Incipient Fluidization of Limestone, Lime, Coal Ash, and Corundum," *Ind. Eng. Chem. Process Des. Dev.*, **20**, 319 (1981).

Ulerich, N. H., Vaux, R. A., Newby, R. A. and Keairns, D. L., Experi-

mental/Engineering Support for EPAs PBC Program, Final Rep., EPA-600/7-80-015A, Westinghouse Research and Development Center, Pittsburgh, PA, USA, Jan. (1980).
Vaux, W. G. and Fellers, A. W., "Measurement of Attrition Tendency in Fluidization," *AIChE Symp. Ser.*, **77**, 107 (1981).
Vaux, W. G. and Schruben, J. S., "Kinetics of Attrition in the Bubbling Zone of Fluidized Beds," *AIChE J.*, **79**, 97 (1978).
Wu, S. Y. and Baeyens, J., "Effect of Operating Temperature on Minimum Fluidization Velocity," *Powder Technol.*, **67**, 217 (1991).
Wu, S. Y. and Chu, C. Y., "Attrition in a Gas Fluidized Bed with Single High Velocities Vertical Nozzle," World Congress on Particle Technology 3rd, Brighton, U.K., 152 (1998).
Wu, S. Y., Baeyens, J. and Chu, C. Y., "Effect of the Grid-Velocity on Attrition in Gas Fluidized Beds," *Can. J. of Chem. Eng.*, **77**, 738 (1999).